

Exact equal time statistics of Orszag–McLaughlin dynamics investigated using the Hopf characteristic functional approach

Ookie Ma and J B Marston

Department of Physics, Box 1843, Brown University, Providence, RI 02912-1843, USA

E-mail: seungwook_ma@physics.brown.edu and marston@physics.brown.edu

Received 19 August 2005

Accepted 22 September 2005

Published 10 October 2005

Online at stacks.iop.org/JSTAT/2005/P10007

[doi:10.1088/1742-5468/2005/10/P10007](https://doi.org/10.1088/1742-5468/2005/10/P10007)

Abstract. By employing Hopf's functional method, we find the exact characteristic functional for a simple nonlinear dynamical system introduced by Orszag. The steady state equal time statistics thus obtained are compared to direct numerical simulation. The solution is both non-trivial and strongly non-Gaussian.

Keywords: rigorous results in statistical mechanics, exact results, turbulence, stationary states (theory)

ArXiv ePrint: [nlin.SI/0506021](https://arxiv.org/abs/nlin.SI/0506021)

Contents

| | |
|--|-----------|
| 1. Introduction | 2 |
| 2. Orszag–McLaughlin dynamical system | 3 |
| 3. Hopf functional approach | 5 |
| 4. Exact characteristic functional | 7 |
| 5. Infinite dimensional limit | 9 |
| 6. Numerical simulation | 10 |
| 7. Discussion | 10 |
| Acknowledgments | 11 |
| References | 11 |

1. Introduction

A nonlinear dynamical system can be completely deterministic and its solution unique, yet two trajectories that begin close to one another may diverge significantly in a finite time. Such sensitive dependence on initial conditions sets a fundamental limit on predictive accuracy, as these systems ‘forget’ their initial conditions after a short time. Probabilistic descriptions, by contrast, avoid the details of time evolution, and instead answer meaningful statistical questions. As a canonical example, experimental measurements of turbulent velocity fluctuations show disordered and unpredictable behaviour yet reproducible statistical properties. The complexity of the flow contrasts with the smoothness of averaged quantities like the energy spectrum, demonstrating that statistical descriptions may be both economical and insightful.

To accumulate statistics, numerical simulations may implement ensemble averages over initial conditions and/or long time integration, yet the computational work required to carry out such calculations can be prohibitive in the case of high dimensional systems. Purely statistical approaches can be quite helpful for such problems. Furthermore, sub-grid physics is often modelled statistically; fewer inconsistencies will arise if all of the dynamical variables are treated statistically from the outset. Finally, from a theoretical perspective it can be more enlightening to work directly with statistical approaches [1].

In this paper we apply a method pioneered by Hopf [2] to determine the exact characteristic functional of a simple chaotic dynamical system introduced by Orszag [3]. Knowledge of the characteristic functional yields all of the equal time moments and offers some advantage over the more common statistical description in terms of the probability density function (PDF). In particular, moment and cumulant expansions arise naturally in the Hopf formalism [4]. Such expansions, however, suffer from the usual closure problem and break down when the statistics are strongly non-Gaussian. The exact solution to Hopf’s equation is both non-trivial and, for a finite number of dimensions, non-Gaussian.

Exact solutions are invaluable as they both yield physical insight and provide important benchmarks against which approximate methods can be tested.

The outline of the paper is as follows. In section 2 we introduce the finite dimensional Orszag–McLaughlin dynamical system. We briefly review the Hopf functional approach in section 3. The exact characteristic functional of the Orszag–McLaughlin system is presented in section 4. In section 5 we consider the limit of large dimension and show that the statistics become Gaussian in this limit. Comparison of the solution against direct numerical simulation is made in section 6. Finally in section 7 we highlight a few points.

2. Orszag–McLaughlin dynamical system

In Orszag’s lecture notes [3] and in a subsequent paper with McLaughlin [5], a finite mode system was introduced as a toy model of inviscid flow:

$$\frac{dx_i}{dt} = x_{i+1}x_{i+2} + x_{i-1}x_{i-2} - 2x_{i+1}x_{i-1}, \quad (1)$$

with $i = 1, \dots, N$ and the periodic boundary condition $x_{i+N} = x_i$. The dimension N can be either even or odd; we focus on odd N here. Like Euler’s equation, the equations of motion (EOM) contain only quadratic terms. The equations resemble those of the shell models of Gledzer, Ohkitani and Yamada (GOY) and of Sabra [6], but the periodic boundary condition would be unphysical in a shell model, as the longest wavelength mode would be coupled to the shortest. Nevertheless, these simple EOM generate complicated chaotic trajectories, as shown in figure 1.

Despite the fact that the Orszag–McLaughlin dynamical system is non-Hamiltonian (trivially so in an odd number of dimensions), it conserves an energy-like quantity in the sense that

$$E = \frac{1}{2} \sum_{i=1}^N x_i^2 \quad (2)$$

is a constant of the motion. Trajectories lie on a hypersphere of radius

$$R = \sqrt{2E}. \quad (3)$$

For odd values of $N \geq 5$, (3) is the only isolating integral of motion [5]. In addition, for $N = 5$, all periodic orbits and fixed points are unstable [5]. The system appears to be ergodic for all initial conditions except a set of measure zero. This also seems to be the case for other odd values of $N > 5$. Finally we note that the dynamical system formally obeys Liouville’s theorem, despite being non-Hamiltonian:

$$\begin{aligned} 0 &= \sum_{i=1}^N \frac{\partial}{\partial x_i} \left(\frac{dx_i}{dt} \right) \\ &= \sum_{i=1}^N \frac{\partial}{\partial x_i} (x_{i+1}x_{i+2} + x_{i-1}x_{i-2} - 2x_{i+1}x_{i-1}). \end{aligned} \quad (4)$$

The assumption of ergodicity combined with the energy constraint (2) has an important consequence. Strikingly, the system exhibits continuous rotational symmetry

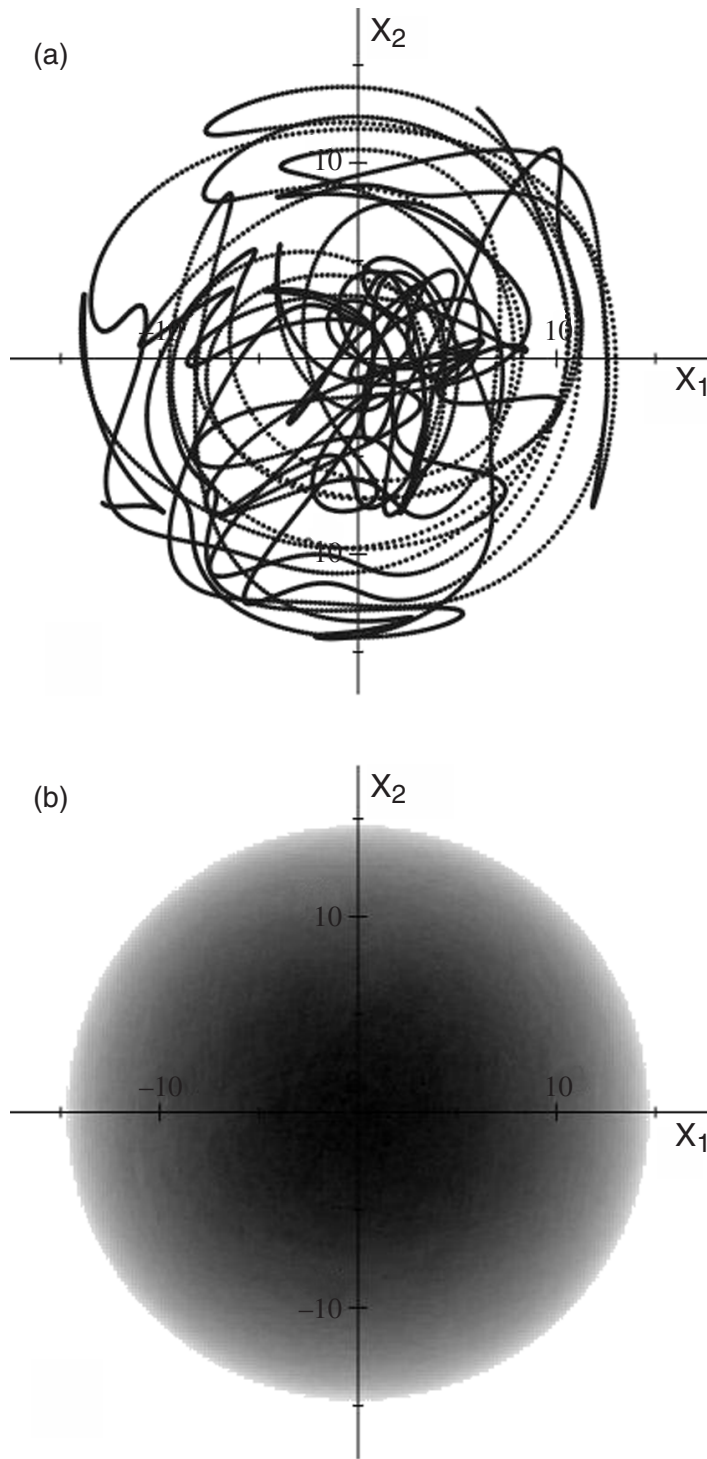


Figure 1. (a) A typical trajectory of the Orszag–McLaughlin dynamical system, for the case $N = 5$, projected onto the x_1 – x_2 plane. Trajectories appear random and lie on the surface of a five-dimensional hypersphere. (b) The probability density function projected onto the x_1 – x_2 plane, as determined by long time integration.

in its statistics, despite the fact that the EOM are invariant only under discrete rotations corresponding to the permutation of indices. The statistics are determined by only a single parameter, the energy E , or equivalently the radius R .

3. Hopf functional approach

Hopf developed a functional method for accessing the equal time statistics of deterministic dynamical systems [2]. Here we briefly review his approach. The reader can find more detailed information in [4].

For the purposes of illustrating the method and applying it in the next section to the Orszag–McLaughlin system, it suffices to consider deterministic dynamical systems described by a set of first-order differential equations:

$$\frac{dx_i}{dt} = F_i(x_1, x_2, \dots, x_N); \quad i = 1, \dots, N. \quad (5)$$

Introduce a set of variables \vec{u} conjugate to the coordinates \vec{x} and a functional Ψ that resembles a wavefunction in quantum mechanics:

$$\Psi[\vec{u}, \vec{x}(t)] \equiv e^{i\vec{u} \cdot \vec{x}(t)}. \quad (6)$$

It then follows from the EOM, (5), that Ψ is governed by a Schrödinger-like equation:

$$i \frac{d\Psi}{dt} = \hat{H}\Psi. \quad (7)$$

Here the Hopf ‘Hamiltonian’ on the right-hand side is the linear operator

$$\hat{H} = - \sum_{j=1}^N u_j F_j \left(\frac{1}{i} \frac{\partial}{\partial u_1}, \frac{1}{i} \frac{\partial}{\partial u_2}, \dots, \frac{1}{i} \frac{\partial}{\partial u_N} \right). \quad (8)$$

Note that \hat{H} is generally non-Hermitian, as there is no requirement (unlike in quantum mechanics) that the time evolution of Ψ be unitary. For instance the inner product, which plays a central role in quantum mechanics, has no particular meaning in the Hopf formalism. We call (7) together with (8) ‘Hopf’s equation’ in the following.

We emphasize that Hopf’s equation is linear even though the EOM may be nonlinear. Therefore—and this is the key point—(7) can be averaged over an ensemble of initial conditions. It is the averaging that blurs the deterministic trajectories and, pursuing the analogy with quantum mechanics, can be thought of as the origin of non-zero \hbar . The corresponding characteristic functional $\overline{\Psi}(\vec{u}, t)$ that solves the Hopf equation is simply an average of $\Psi[\vec{u}, \vec{x}(t)]$ over initial conditions at time $t = 0$:

$$\begin{aligned} \overline{\Psi}(\vec{u}, t) &= \overline{e^{i\vec{u} \cdot \vec{x}(t)}} \\ &= \int_{-\infty}^{\infty} e^{i\vec{u} \cdot \vec{x}(t)} P(\vec{x}(0)) d^N x(0). \end{aligned} \quad (9)$$

For notational simplicity we eliminate the bar over $\overline{\Psi}$ in the following.

It is readily seen that derivatives of the characteristic functional yield the equal time moments:

$$\frac{1}{i} \frac{\partial \Psi(\vec{u}, t)}{\partial u_j} \Big|_{\vec{u}=0} = \int_{-\infty}^{\infty} x_j(t) P(\vec{x}(0)) d^N x(0) = \overline{x_j(t)}, \quad (10)$$

$$-\frac{\partial^2 \Psi(\vec{u}, t)}{\partial u_j \partial u_k} \Big|_{\vec{u}=0} = \int_{-\infty}^{\infty} x_j(t) x_k(t) P(\vec{x}(0)) d^N x(0) = \overline{x_j(t) x_k(t)}, \quad (11)$$

and so on. All conjugate coordinates \vec{u} are taken to zero after the derivatives are calculated. From (9) it is clear that the characteristic functional is simply the Fourier transform of the PDF, and one uniquely determines the other. We note that the calculated n -point correlation functions are more simply extracted from the characteristic functional than from the PDF. In the case of the PDF we must integrate over all of the coordinates. For the characteristic functional all that is required is the calculation of some derivatives followed by setting all of the conjugate coordinates to zero [7]. The advantage is particularly clear in the case of infinite dimensional problems such as fluid flow for which the velocity field is a continuous function of position.

Of special importance are zero-mode characteristic functionals that satisfy $\hat{H}\Psi_0 = 0$. The zero-mode plays a role as important as the ground state in quantum mechanics as it encodes information about the steady state behaviour of the dynamical system. In the following, we employ Dirac's bracket notation $\langle \dots \rangle$ to indicate steady state statistical averages.

In order for Ψ to be a valid characteristic functional, it must obey two general boundary conditions that follow directly from equation (9):

$$\Psi(\vec{0}) = 1 \quad (12)$$

and

$$\lim_{|\vec{u}| \rightarrow \infty} \Psi(\vec{u}) = 0. \quad (13)$$

Furthermore, a necessary and sufficient condition for ensuring semi-positivity of the PDF is specified by Bochner's theorem [8]:

$$\int d^N u d^N u' \phi(\vec{u}) \Psi(\vec{u} - \vec{u}') \phi^*(\vec{u}') \geq 0 \quad (14)$$

for all complex-valued test functions $\phi(\vec{u})$. This constrains all of the equal time moments or cumulants. For example, even cumulants cannot be negative [9, 10]. Additional boundary conditions arise from conservation laws. In particular, for the Orszag–McLaughlin system, conservation of energy imposes an infinite set of boundary conditions:

$$\left(-\vec{\nabla}_u^2\right)^n \Psi \Big|_{\vec{u}=0} = (2E)^n \quad (15)$$

for all integer n .

For completeness, we conclude this brief review of the Hopf functional approach by discussing the inclusion of random forcing. For simplicity, consider the introduction of

Gaussian random forcing f_i , δ -correlated in time, and with zero mean. The EOM are modified to read

$$\frac{dx_i}{dt} = F_i(\vec{x}) + f_i(t) \quad (16)$$

where

$$[f_j(t)] = 0, \quad (17)$$

$$[f_j(t)f_k(t')] = 2\Gamma\delta_{jk}\delta(t-t') \quad (18)$$

and the square brackets $[\dots]$ denote an average over the random variable. The Hopf equation for the characteristic functional now reads [11]

$$i\frac{\partial\Psi(\vec{u}, t)}{\partial t} = \left(\vec{u} \cdot \vec{F}(-i\vec{\nabla}_u) - i\Gamma|\vec{u}|^2\right) \Psi(\vec{u}, t). \quad (19)$$

One possible derivation of (19) begins with the better-known Fokker–Planck equation [12]:

$$\frac{\partial P(\vec{x}, t)}{\partial t} = \left(-\vec{\nabla}_x \cdot \vec{F}(\vec{x}) + \Gamma\nabla_x^2\right) P(\vec{x}, t). \quad (20)$$

The Hopf equation (19) is recovered upon making the duality transformation $x_j \rightarrow (1/i)(\partial/\partial u_j)$ and $(\partial/\partial x_j) \rightarrow (1/i)u_j$. The duality transformation respects the commutation relation between the conjugate coordinates: $[x_j, (1/i)u_k] = \delta_{jk}$. Thus the Hopf and Fokker–Planck approaches are seen to be equivalent, and dual to one another, yet the inclusion of random forcing seems more intuitive in the latter case. As is well known, the first term in the Fokker–Planck equation is a statement of conservation of phase-space density. The second is a diffusion term due to random forcing, which smears out an initially sharp distribution. Pawula [13] showed that Gaussian random forcing leads to only a finite number of terms in the Fokker–Planck equation. If the forcing is non-Gaussian, the Fokker–Planck equation must include an infinite set of terms involving derivatives higher than two.

4. Exact characteristic functional

The Hopf Hamiltonian for the Orszag–McLaughlin dynamical system follows directly from (1) and (8):

$$\hat{H} = \sum_{i=1}^N u_i \left(\frac{\partial^2}{\partial u_{i+1} \partial u_{i+2}} + \frac{\partial^2}{\partial u_{i-1} \partial u_{i-2}} - 2 \frac{\partial^2}{\partial u_{i+1} \partial u_{i-1}} \right) \quad (21)$$

where periodic boundary conditions $\partial/\partial u_{i+N} = \partial/\partial u_i$ are implied. For this particular system the Hamiltonian is Hermitian, though (as noted above) this will not always be the case for other dynamical systems.

It is straightforward to show that any $\Psi(\vec{u})$ that is a function purely of the magnitude of \vec{u} is a zero-mode of the above \hat{H} . This is consistent both with the assumption of ergodicity and with the numerical simulation of the PDF illustrated in figure 1. However, such zero-modes are, in general, a superposition of states of different energies (15).

Imposition of the energy constraint (15) picks out the desired solution. Consider a Taylor series expansion of Ψ_0 in the dimensionless parameter $(R|\vec{u}|)^2$:

$$\Psi_0(\vec{u}) = \sum_{\ell=0}^{\infty} b_{\ell} (R|\vec{u}|)^{2\ell}. \quad (22)$$

The series coefficients can be found by observing that the energy constraint requires

$$R^{2\ell} = \langle |\vec{x}|^{2\ell} \rangle, \quad (23)$$

and, furthermore, the moments may be expressed in terms of the coefficients b_{ℓ} . For example, successive differentiation of (22) reveals that

$$\langle x_1^4 \rangle = 4! b_2 R^4 \quad (24)$$

and

$$\langle x_1^2 x_2^2 \rangle = 2 \cdot 2! \cdot 2! b_2 R^4. \quad (25)$$

Combining this with the energy constraint

$$\begin{aligned} R^4 &= N \langle x_1^4 \rangle + 2 \binom{N}{2} \langle x_1^2 x_2^2 \rangle \\ &= N 4! b_2 R^4 + 2^2 \binom{N}{2} 2! 2! b_2 R^4 \end{aligned} \quad (26)$$

yields

$$b_2 = \frac{1}{N 4! + 2^2 \binom{N}{2} 2! 2!}. \quad (27)$$

Each coefficient can be determined in this manner. The series so generated is

$$\Psi_0(\vec{u}) = \Gamma(N/2) \sum_{\ell=0}^{\infty} \frac{1}{\Gamma(\ell + N/2)} \frac{(-1)^{\ell}}{2^{2\ell} \ell!} (R|\vec{u}|)^{2\ell}. \quad (28)$$

The series may be summed into the Bessel function $J_{N/2-1}$:

$$\Psi_0(\vec{u}) = \Gamma(N/2) (R|\vec{u}|/2)^{1-N/2} J_{N/2-1}(R|\vec{u}|). \quad (29)$$

We note that the exact zero-mode characteristic functional satisfies the boundary conditions, (12) and (13).

The characteristic zero-mode may be approached from another direction, one that does not rely upon series expansion. Knowing that the trajectories are distributed uniformly on the hypersphere's surface, the stationary PDF is a simple δ -function shell:

$$P(\vec{x}) = \frac{1}{S_{N-1}} \delta(|\vec{x}| - R) \quad (30)$$

where R is given by (3). The normalization factor S_{N-1}^{-1} is simply the inverse of the total surface area of the hypersphere. By direct substitution it can be seen that this is a zero-mode solution to the Fokker–Planck (20). Now Ψ_0 may be obtained from the Fourier transform of (30). Due to the spherical symmetry it is most convenient to work in

spherical coordinates. The N Cartesian coordinates are related to spherical coordinates by

$$\begin{aligned} x_1 &= r \sin \phi_0 \prod_{j=1}^{N-2} \sin \phi_j \\ x_2 &= r \cos \phi_0 \prod_{j=1}^{N-2} \sin \phi_j \\ x_3 &= r \cos \phi_1 \prod_{j=2}^{N-2} \sin \phi_j, \quad \text{etc.} \end{aligned} \quad (31)$$

In these coordinates the volume element is

$$dV = \prod_{j=1}^N dx_j = r^{N-1} dr \prod_{j=0}^{N-2} \sin^j \phi_j d\phi_j. \quad (32)$$

By exploiting spherical symmetry, we obtain the characteristic functional (29):

$$\begin{aligned} \Psi_0(\vec{u}) &= \frac{1}{S_{N-1}} \int e^{i\vec{u}\cdot\vec{x}} \delta(|\vec{x}| - R) dV \\ &= \Gamma(N/2) (R|\vec{u}|/2)^{1-N/2} J_{N/2-1}(R|\vec{u}|). \end{aligned} \quad (33)$$

Because Ψ_0 is the Fourier transform of a non-negative PDF, it automatically satisfies Bochner's theorem (14).

5. Infinite dimensional limit

We now show that the statistics are Gaussian in the limit of high dimension. Consider the expansion (28). In the limit $N \rightarrow \infty$, the Taylor series approaches that of a Gaussian:

$$e^{-u^2/2} = \sum_{l=0}^{\infty} \frac{(-1)^l}{2^{2l} l!} u^{2l}. \quad (34)$$

Alternatively, we may integrate the PDF over all but the last Cartesian coordinate:

$$P(x_N) = \frac{R S_{N-2}}{S_{N-1}} \left(1 - \left(\frac{x_N}{R} \right)^2 \right)^{N-4}; \quad |x_N| \leq R. \quad (35)$$

Since

$$\lim_{N \rightarrow \infty} \left(1 - \left(\frac{x_N}{R} \right)^2 \right)^{N-4} = e^{-(N-4)(x_N/R)^2}, \quad (36)$$

a Gaussian distribution is recovered at large N . For finite N , the projected PDF is highly non-Gaussian for $|x_N|$ comparable to R ; unlike a Gaussian it vanishes when $|x_N| \geq R$. As N is increased, however, the projected PDF becomes increasingly narrow with a width of $\mathcal{O}(R/\sqrt{N})$, and cannot be distinguished from a Gaussian even for $|x_N|$ of order R .

The fact that a Gaussian distribution appears in the limit $N \rightarrow \infty$ is not unexpected. Motion along a single coordinate is governed by the essentially random values of the remaining $N-1$ coordinates. The central limit theorem then applies, resulting in Gaussian statistics.

Table 1. A comparison of low order moments, scaled by R , as calculated from the exact characteristic functional and from time averages obtained by direct numerical simulation. Numerical integrations were performed using the second-order Runge–Kutta algorithm. Here $R = 17.3$, and the averages are calculated over time intervals of duration $t_1 = 100$ and $t_2 = 10\,000$. Note the convergence of the numerical results to the analytical values as the length of the time integration increases.

| Moments | Prediction | Simulation 1 | Simulation 2 |
|-------------------------------------|-------------------------------|--------------|--------------|
| $\langle x_1 \rangle / R$ | 0 | 0.000 610 | 0.000 0823 |
| $\langle x_1^2 \rangle / R^2$ | $\frac{1}{5} = 0.2$ | 0.201 | 0.200 |
| $\langle x_1 x_2 \rangle / R^2$ | 0 | −0.001 65 | −0.000 211 |
| $\langle x_1^3 \rangle / R^3$ | 0 | 0.000 505 | 0.000 0945 |
| $\langle x_1^2 x_2 \rangle / R^3$ | 0 | −0.000 209 | −0.000 0171 |
| $\langle x_1^4 \rangle / R^4$ | $\frac{3}{35} \approx 0.0857$ | 0.086 6 | 0.085 7 |
| $\langle x_1^2 x_2^2 \rangle / R^4$ | $\frac{1}{35} \approx 0.0286$ | 0.028 2 | 0.028 6 |

6. Numerical simulation

Finally we make a quantitative comparison with direct numerical simulation. To be definite, consider the $N = 5$ case. The characteristic functional (29) in this specific case reduces to

$$\Psi_0(\vec{u}) = 3 \frac{\sin(R|\vec{u}|) - R|\vec{u}| \cos(R|\vec{u}|)}{R^3 |\vec{u}|^3} \quad (37)$$

or in series form (28) to

$$\Psi_0(\vec{u}) = 1 - \frac{R^2 |\vec{u}|^2}{10} + \frac{R^4 |\vec{u}|^4}{280} - \frac{R^6 |\vec{u}|^6}{15\,120} + \dots \quad (38)$$

Table 1 shows that there is good agreement between moments calculated by successive differentiation of the exact characteristic functional (37) and the time-averaged values obtained from direct numerical simulation. Likewise (35) gives the projected PDF for the single coordinate x_5 :

$$P(x_5) = \begin{cases} \frac{3}{4R} - \frac{3x_5^2}{4R^3}, & x_5 \leq R \\ 0, & x_5 > R. \end{cases} \quad (39)$$

Figure 2 compares this function with the normalized histogram generated from a direct numerical simulation. Again there is good agreement.

7. Discussion

We employed the Hopf characteristic functional approach to study the statistics of the deterministic Orszag–McLaughlin system. The system is simple enough, with emergent

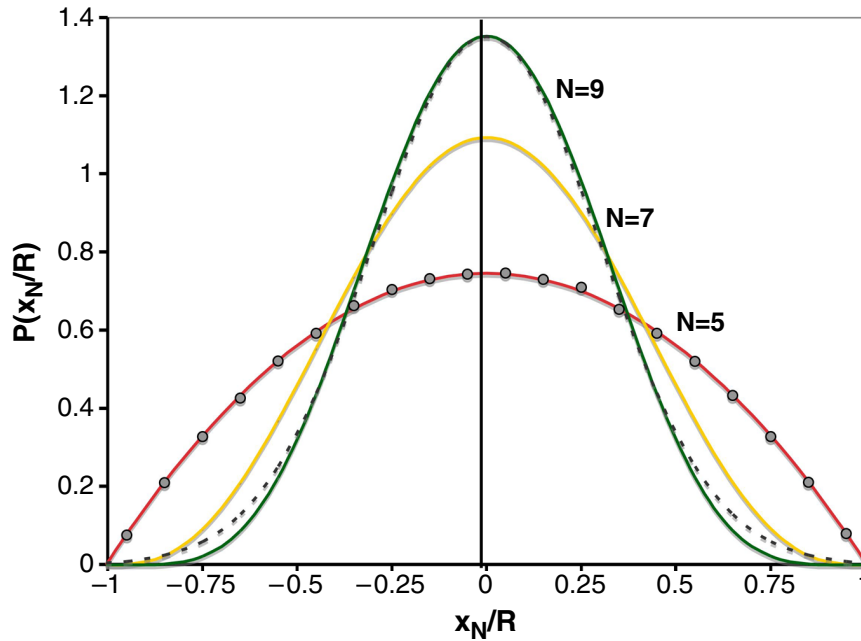


Figure 2. PDF projected onto a single coordinate. The dots are from direct numerical simulation of the $N = 5$ system; solid lines are plots of (35) for $N = 5, 7$ and 9 , showing the approach to Gaussian statistics as N becomes large, and the dashed line is a normalized Gaussian with height equal to the $N = 9$ PDF.

spherical symmetry in the statistics, that the exact characteristic zero-mode can be found. The equal time statistics so obtained are non-Gaussian and are in good agreement.

Exact solutions serve as rigorous illustrations of physical principles and as benchmarks against which approximate solutions can be checked. For instance, in the case of the Orszag–McLaughlin system, a cumulant expansion carried out to third order reproduces the exact first to third cumulants (only the second cumulants are non-zero), yet higher order cumulants are by definition zero. Inspection of (38) immediately reveals the size of the errors so incurred. The development of more sophisticated, non-perturbative, methods to address the non-equilibrium statistical mechanics of dynamical systems can likewise benefit from tests against such exact solutions.

Acknowledgments

We thank Bernd Braunecker, Matt Hastings and Peter Weichman for helpful discussions. This work was supported in part by the National Science Foundation under grant No DMR-0213818.

References

- [1] Lorenz E, 1967 *The Nature and Theory of the General Circulation* (Geneva: World Meteorological Organization)
- [2] Hopf E, *Statistical hydromechanics and functional calculus*, 1952 *J. Ratl. Mech. Anal.* 1 87

- [3] Orszag S A, *Lectures on the Statistical Theory of Turbulence*, 1977 *Fluid Dynamics, Les Houches 1973* ed R Baillan and J L Peube (New York: Gordon and Breach)
- [4] Frisch U, 1995 *Turbulence The Legacy of A.N. Kolmogorov* (Cambridge: Cambridge University Press)
- [5] Orszag S A and McLaughlin J B, *Evidence that random behavior is generic for nonlinear differential equations*, 1980 *Physica D* **1** 68
- [6] Biferale L, *Shell models in turbulence*, 2003 *Annu. Rev. Fluid Mech.* **35** 441
- [7] Monin A S and Yaglom A M, 1971 *Statistical Fluid Mechanics: Mechanics of Turbulence* (Cambridge, MA: MIT Press)
- [8] Bochner S, *Monotone Funktionen, Stieltjessche Integrale und Harmonische Analyse*, 1933 *Math. Ann.* **108** 378
- [9] Kraichnan R H, *Realizability inequalities and closed moment equations*, 1980 *Ann. New York Acad. Sci.* **357** 37
- [10] Hanggi P and Talkner P A, *A remark on Truncation schemes of Cumulant hierarchies*, 1980 *J. Stat. Phys.* **22** 65
- [11] Novikov E A, *Functionals and the random-force method in turbulence*, 1964 *Sov. Phys. JETP* **20** 1290
- [12] Risken H, 1996 *The Fokker–Planck Equation: Methods of Solution and Applications* 2nd edn (Berlin: Springer)
- [13] Pawula R F, *Approximation to the linear Boltzmann equation by the Fokker–Planck equation*, 1967 *Phys. Rev.* **162** 186